HHS Public Access

Author manuscript

J Porphyr Phthalocyanines. Author manuscript; available in PMC 2016 January 01.

Published in final edited form as:

J Porphyr Phthalocyanines. 2015 ; 19(1-3): 352–360. doi:10.1142/S108842461550025X.

Reactions of a heme-superoxo complex toward a cuprous chelate and •$NO_{(g)}$: C*c*O and NOD chemistry

Savita K. Sharma, **Patrick J. Rogler**, and **Kenneth D. Karlin**[*,✧]

Department of Chemistry, Johns Hopkins University, Baltimore, MD 21218, USA

Abstract

Following up on the characterization of a new (heme)Fe^{III}-superoxide species formed from the cryogenic oxygenation of a ferrous-heme (P^{Py})Fe^{II} (**1**) (P^{Py} = a tetraarylporphyrinate with a covalently tethered pyridine group as a potential axial base), giving (P^{Py})Fe^{III}-$O_2^{\bullet-}$ (**2**) (*Li Y et al., Polyhedron* 2013; **58**: 60–64), we report here on (i) its use in forming a cytochrome *c* oxidase (C*c*O) model compound, or (ii) in a reaction with nitrogen monoxide (•NO; nitric oxide) to mimic nitric oxide dioxygenase (NOD) chemistry. Reaction of (**2**) with the cuprous chelate [Cu^{I}(AN)][$B(C_6F_5)_4$] (AN = bis[3-(dimethylamino) propyl]amine) gives a *meta*-stable product [(P^{Py})Fe^{III}-(O_2^{2-})-Cu^{II}(AN)][$B(C_6F_5)$4] (**3a**), possessing a high-spin iron(III) and Cu(II) side-on bridged peroxo moiety with a μ-η^2:η^2-binding motif. This complex thermally decays to a corresponding μ-oxo complex [(P^{Py})Fe^{III}-(O^{2-})-Cu^{II}(AN)][$B(C_6F_5)$4] (**3**). Both (**3**) and (**3a**) have been characterized by UV-vis, ^{2}H NMR and EPR spectroscopies. When (**2**) is exposed to •$NO_{(g)}$, a ferric heme nitrato compound forms; if 2,4-di-*tert*-butylphenol is added prior to •$NO_{(g)}$ exposure, phenol *ortho*-nitration occurs with the iron product being the ferric hydroxide complex (P^{Py})Fe^{III}(OH) (**5**). The latter reactions mimic the action of NOD's.

Keywords

heme-superoxo; high spin heme-copper peroxo; heme-copper-μ-oxo; peroxynitrite; nitrate

INTRODUCTION

Metalloenzymes form an essential component of the various biological and physiological functions that are essential for life [1]. Hemoproteins are perhaps the best-known class of metalloenzymes, and their reactions with dioxygen are foundational to aerobic life. These proteins are critical to dioxygen storage and transport (myoglobin and hemoglobin) [2], substrate oxygenation (cytochrome P-450 family), as well as dioxygenation [3] and peroxidation [4]. Heme-copper proteins are critical to cellular respiration (*e.g.* in cytochrome *c* oxidase). Nitric oxide is biosynthesized and interacts with hemoproteins as part for this molecule's involvement in inflammatory responses, cellular signaling, and

[*]Correspondence to: Kenneth D. Karlin, karlin@jhu.edu.

[✧]SPP full member in good standing

vasodilation. Nitric oxide dioxygenase (NOD) [5] and nitric oxide reductase (NOR) [6] enable cellular NO regulation/removal when it is present in excess.

It has been shown that C*c*O functionality is inhibited in the presence of NO [7, 8] *via* competition with O_2 for binding at the binuclear center. Under certain physiological conditions the NO concentration *in vivo* can reach levels that significantly affect the reaction rate of C*c*O [9]. To compensate, myoglobin (Mb) and/ or hemoglobin (Hb) play a major role in scavenging •NO, helping to keep respiratory homeostasis. This maintains the proton gradient over the mitochondrial inner membrane, driving ATP synthesis. When •NO is overproduced *in vivo* as a component of inflammatory response, reactive nitrogen species (RNS) can be formed by the reaction of NO with reactive oxygen species (ROS) such as superoxide, to generate a peroxynitrite ($O{=}NOO^-$). Peroxynitrite [10, 11] is a strong oxidant and nitrating agent, and reacts with a number of biological substrates such as thiols [12], tyrosine residues [13], lipids, CO_2, DNA [14–16] and metalloproteins [17]. Hence, •NO and peroxynitrite scavenging by Hb/Mb, is critical not only to respiration, but also for the mitigation of oxidative damage *via* NOD activity [18, 19].

Our own research group is particularly interested in providing basic coordination chemistry insights into the possible reactive intermediates formed during C*c*O turnover by using synthetic functional models [20–24]. C*c*O is responsible for the reduction of O_2 to water as a terminal step of the respiratory chain of mitochondria and many aerobic bacteria [25–27]. A ferric superoxo species is the most well studied dioxygen intermediate generated upon initial O_2-reaction with the fully reduced activesite heme Fe(II)–Cu(I) center [28]. This species forms prior to O–O bond cleavage and as such has attracted considerable interest [29–31]. Here, we describe the reactivity of an iron(III)-superoxo species (**2**) towards (i) a cuprous-chelated complex [CuI(AN)][B(C6F5)4] and (ii) •NO, these reactions representing synthetic functional models for C*c*O and NOD, respectively.

RESULTS AND DISCUSSION

Reactivity of the iron(III)-superoxo complex (2) towards $[Cu^I(AN)][B(C_6F_5)_4]$

Earlier work in our group [31] described the synthesis and characterization of $(P^{Py})Fe^{II}$ (**1**) [(P^{Py}) = pyridyl tailed porphyrinate (2-)] (λ_{max} = 416, 525, 554 (sh) nm) which reacts reversibly with dioxygen to give a diamagnetic iron(III)-superoxo species $(P^{Py})Fe^{III}$-($O_2^{\bullet-}$) (**2**) (UV-vis, λ_{max}= 419, 535 nm; EPR, silent). This is stable in solution below −30 °C in coordinating solvents such as tetrahydrofuran (THF), acetone, or acetonitrile as well as in non-coordinating solvents like dichloromethane (DCM). The use of copper ion complexes with tridentate alkylamino ligand AN has previously been useful [23, 32–34] and as such this copper chelate was employed here. Addition of one equivalent of $[Cu^I(AN)][B(C_6F_5)_4]$ (Scheme 1) to the superoxo compound (**2**) in THF at −100 °C, monitored by UV-vis spectroscopy, leads to the immediate formation of a heme-copper-O_2 adduct (**3a**) [λ_{max} = 420, 530, 555 (sh) nm], see Fig. 1. The UV-vis spectrum of (3a) is very similar to our previously described high-spin $[(heme)Fe^{III}\text{-}(O_2^{2-})\text{-}Cu^{II}(L)]^+$ species where L is a tri- or tetradentate alkylamino or pyridylalkylamino ligand; these possess a side-on binding of peroxide to both metal ions, as depicted in Scheme 1 [35–37]. Thermal decomposition of

(**3a**) leads to the formation of complex (**3**) with a red shifted Soret band at 443 nm and Q-band at 556 nm (Fig. 1). These are characteristic features for μ-oxo Fe^{III}-O-Cu^{II} like species, such as the previously structurally and spectroscopically characterized complex [$(F_8)Fe^{III}$-(O_2^-)-Cu^{II}(TMPA)]$^+$ [38] (TMPA = tris(2-pyridylmethyl)amine). Complex (**3**) can also be obtained by direct bubbling of dioxygen to a 1:1 mixture of (P^{Py}) Fe^{II} (**1**) and [Cu^I(AN)] [$B(C_6F_5)_4$] at −80 °C in THF. The μ-oxo complex [(P^{Py})Fe^{III}-(O_2^-)-Cu^{II}(AN)]$^+$ (**3**) (or rather a protonated μ-hydroxo conjugate acid form), are of interest since such species derive from dioxygen reactivity, thus perhaps related to C*c*O reaction chemistry [39, 40].

Further characterization of μ-oxo complex (**3**) was provided by low temperature 2H NMR spectroscopy of the pyrrole deuterated analogue of (P^{Py})FeII (**1**), (d_8-P^{Py}) Fe^{II}. Figure 2 shows ^{2}H NMR spectra of the oxygenation reaction of a (P^{Py})Fe^{II}-THF (1) exhibits a pyrrole resonance at † 10 ppm, indicative of a low-spin (S = 0) six-coordinate ferrous heme at low temperature, but we also observe pyrrole resonances at † 98 and 86 ppm, which are characteristic of a penta-coordinated high spin heme. We interpret this observed NMR spectroscopic data as indicating that complex (**1**) is a mixture of 6-coordinate (pyridyl + THF) low-spin iron(II) and 5 or 6-coordinate high-spin iron(II) (*e.g.* pyridyl arm off, THF bound, or *vice versa*, and also possibly a bis-THF ligated ferrous heme). Direct bubbling of dioxygen to (1) gives superoxo complex (**2**) where a pyrrole resonance occurs in the diamagnetic region, at † 9.0 ppm. Subsequent addition of one equiv. of [Cu^I(AN)]$^+$ to the cold solution of superoxo complex (**2**) in an NMR tube leads to the formation of [(P^{Py})Fe^{III}-(O^{2-})-Cu^{II}(AN)]$^+$ (**3**), with a downfield shifting of the pyrrole resonance to † 102 ppm (Fig. 2), indicative of a high-spin ferric heme (also, see below). Complex (**3**) is stable at room temperature. We have previously reported this characteristic pattern of a downfield shifted pyrrole resonance for (P)Fe^{III}-X-Cu^{II} (X = O_2^{2-} or O^{2-}) systems having overall S = 2 spin states [37, 41–43], which arise from the antiferromagnetic coupling of the S = 5/2 high-spin heme-Fe(III) center to an S = ½ copper(II) moiety, through the bridging X ligand in (**3**) or (**3a**). When monitoring peroxo complex (**3a**) by ^{2}H NMR spectroscopy, a clean thermal transformation to (**3**) is observed. EPR spectroscopic interrogation of (**3**) and (**3a**) revealed that both are EPR inactive, consistent with their formulations.

Reactivity of iron(III)-superoxo complex (2) towards •$NO_{(g)}$

Using a gas-tight three way syringe, addition of •$NO_{(g)}$ to superoxo species (P^{Py})Fe^{III}-$(O_2^{\bullet-})$ (**2**) at −80 °C in THF, as monitored by UV-vis spectroscopy, led to the immediate formation of a five-coordinate nitrato compound (P^{Py}) Fe^{III}-(ONO_2) (**4**) [UV-vis, λ_{max} = 397, 410 (sh), 505, 573, 650 nm; EPR, g = 6, 14 K, high-spin iron(III)], as indicated in Scheme 2 and with spectra shown in Fig. 3. Product (**4**) yields a positive test for nitrate ion, as determined using semiquantitative QUANTOFIX nitrate (NO_3^-)/nitrite (NO_2^-) test paper; no NO_2^- ion was detected and the yield of nitrate ion was estimated to be > 75% (see Experimental). These results are very similar to what we observed in a previous study of (F_8) Fe^{II} (F_8 = tetrakis(2,6-difluorophenyl)porphyrinate(2-)) where addition of •$NO_{(g)}$ to the superoxo complex (F8) Fe^{III}-$(O_2^{\bullet-})$, yields a five-coordinate nitrato heme complex [44]. While no transient species were detected following addition of •$NO_{(g)}$ to (**2**) and isolation of (**4**), the formation of a nitrite complex supports the intermediacy of a peroxynitrite $^-$OON=O species

(**4a**) which formed during the reaction (Scheme 2), indicating an NOD type of reaction mechanism (see below).

Thus, we sought chemical evidence which might support our supposition involving the formation of a peroxynitrite species during the reaction of (**2**) with •$NO_{(g)}$. Here, a tyrosine analog, 2,4-di-*tert*-butylphenol (DTBP), was added into the solution of superoxo complex (P^{Py})Fe^{III}-($O_2^{\bullet-}$) (2). When •$NO_{(g)}$ was subsequently added, we observed the immediate formation of (P^{Py}) Fe^{III}(OH) (5) [λ_{max}= 400, 563 nm] as indicated by the Q-band feature in the UV-vis spectrum (Fig. 4). We then isolated the pure (P^{Py})Fe^{III}(OH) (**5**) (λ_{max}= 410, 563) from this mixture (see Experimental). An authentic sample of (P^{Py})Fe^{III}(OH) (5) (λ_{max}= 412, 563) was prepared (see Experimental), and has nearly identical UV-vis features as those observed for the reaction product. The UV-vis and EPR spectroscopic features observed here also closely match those known for (F_8)Fe^{III}(OH) (λ_{max} = 408, 572 nm high-spin, EPR, g = 6.0) [44] (Fig. 4). Workup of the reaction solution revealed that the product (5) forms along with high yields (>85%) of 2,4-di-*tert*-butyl-6-nitrophenol (NO_2-DTBP), as confirmed *via* gaschromatography. This reaction mixture was also tested for the presence of any NO_3^-/NO_2^- ions and yielded a negative result for both.

These studies indicate the involvement of a hemeperoxynitrite like intermediate [(P^{Py})Fe^{III}-OONO] (**4a**), which we could not detect, but that formed when superoxo complex (P^{Py})Fe^{III}-($O_2^{\bullet-}$) (**2**) was reacted with •$NO_{(g)}$ (Scheme 2). There were previous reports that suggested the detection of heme-peroxynitrite species in the reaction of oxy-heme (*i.e.* ferric superoxo) with •NO(g), either via UV-vis or EPR spectroscopy [18, 45]. However these results were refuted by Moënne-Loccoz and co-workers [46] using rapid freeze quench resonance Raman spectroscopy with Mb, which revealed that such intermediates were in fact iron-bound nitrate species formed prior to their decay to metMb. Still, the generally accepted mechanism of •NO dioxygenase involves direct reaction of the Fe^{III}-($O_2^{\bullet-}$) oxy complex with •NO, giving a peroxynitrite intermediate. Subsequent homolytic O–O bond cleavage produces an oxo-ferryl (Fe^{IV}=O) species and the free radical nitrogen dioxide (•NO_2); the latter attacks the ferryl O-atom to produce a N–O bond, yielding nitrate [47–50]. Recent work with oxy-coboglobin models [51, 52] exhibiting NODlike activity has led to the detection of peroxynitrite intermediates using low temperature FTIR, this work has helped to shed light onto favorable conditions for generating peroxynitrite intermediates. Also, recent work by Nam and Karlin [53] has shown an alternative method for mimicking NOD activity that is isoelectronic to the methods discussed above. In this case, NOD activity was exhibited using a nitrosonium ion added to a non-heme iron peroxo species. Following these literature precedents, we can hypothesize that (**4a**) undergoes homolysis to give a ferryl + •NO_2 radical, which can be captured by phenol present in solution. The ferryl would oxidize the phenol to a phenoxyl radical which will further react with •NO_2 to give *ortho*-nitration of the phenol and form a very stable ferric hydroxo complex (**4**), as we observed (Scheme 2).

EXPERIMENTAL

General

All reagents and solvents used were of commercially available analytical quality except as noted. Dioxygen was dried by passing through a short column of supported P_4O_{10} (Aquasorb, Mallinkrodt). Nitrogen monoxide (•NO) gas was obtained from Matheson Gases (High Purity Grade, Full cylinder ~500 psig @ 70 °F) and purified as follows: it was first passed through multiple columns containing Ascarite II (Thomas Scientific) to remove higher nitrogen oxide impurities. Further purification by distillation was completed by warming frozen •NO (as crystalline N_2O_2) from 78 K in a liquid N_2 cooled vacuum trap to 193 K through use of an acetone/dry-ice (−78 °C) bath, and collection in a second liquid N2 cooled evacuated vacuum trap. This secondary flask was again warmed to 193 K and the purified •NO was collected in an evacuated Schlenk flask (typically 50 mL) closed with a rubber septum secured tightly by copper wire. The •NO in the Schlenk flask is collected and kept at higher pressures (<1 atm). Addition of •NO and O_2 to the metal complex solutions was accomplished using a three-way long needle syringe connected to a Schlenk line.

THF and Pentane were distilled over Na/benzophenone ketyl or calcium hydride. 2,4-di-*tert*-butylphenol (DTBP) was purchased from Sigma-Aldrich and purified by multiple recrystallizations in toluene under Ar. All other reagents were used as received.

Preparation and handling of air-sensitive compounds were performed under an argon atmosphere using standard Schlenk techniques or in an MBraun Labmaster 130 inert atmosphere (<1 ppm O_2, <1 ppm H_2O) drybox filled with nitrogen gas. Solvents were purged with Ar prior to use. All UV-vis measurements were carried out by using a Hewlett Packard 8453 diode array spectrophotometer with a 10 mm path quartz cell. The spectrometer was equipped with HP Chemstation software and a Unisoku thermostated cell holder for low temperature experiments. All NMR spectra were recorded in 7 inch, 5 mm o.d. NMR tubes. Low-temperature 2H NMR (Bruker 300 MHz spectrometer equipped with a tunable deuterium probe to enhance deuterium detection) measurements were performed at −80 °C under a N_2 atmosphere. The ^2H chemical shifts are calibrated to natural abundance deuterium solvent peaks. EPR measurements of the frozen solutions were carried out at 14K on an X-Band Bruker EMX CW EPR spectrometer controlled with a Bruker ER 041 XG microwave bridge operating at the X-band (~9 GHz). Gas chromatography (GC) was performed on an Agilent 6890 gas chromatograph fitted with a HP-5 (5%-phenyl)-methylpolysiloxane capillary column (30 m * 0.32 mm * 0.25 mm) and equipped with a flame-ionization detector.

Synthesis

$(P^{Py})Fe^{II}/(d_8\text{-}P^{Py})Fe^{II}$ (**1**) and $[Cu^{I}(AN)]BAr^{F}$ were synthesized as previously described [31, 32].

Preparation of ^2H NMR and EPR samples *In-situ* generation of complexes (3a) and (3).—In a typical experiment, 0.57 mL of a $(d_8\text{-}P^{Py})Fe^{II}$ (5 mM) solution in THF was placed in a 5 mm rubber septum capped NMR tube. After cooling down the NMR tube to

−80 °C (acetone/N2(liq) bath), dioxygen was bubbled through the solution mixture to form the (d_8-P^{Py}) $Fe^{III}(O_2^{\bullet-})$ complex (**2**). The NMR tube was transferred rapidly into the NMR instrument which was precooled to −85 °C. Similar to our UV-vis experiments, complex (**3a**) was prepared by removing any excess of dioxygen by vacuum/Ar cycles from (**2**) and careful addition of 1 equiv. of [CuI(AN)]BArF complex. Finally, Complex (**3a**) was warmed to RT to obtain decomposed product (**3**). EPR samples were prepared in a similar way by using 9 mm EPR tube.

In-situ generation of complex (4)—In a typical experiment, 0.650 mL of (P^{Py})Fe^{II} (1 mM) in THF was placed in a 9 mm rubber septum capped EPR tube. After cooling down the EPR tube to −80 °C (acetone/N_2(liq) bath), 3 mL dioxygen was bubbled through the solution mixture to form the (P^{Py})$Fe^{III}(O_2^{\bullet-})$ complex (**2**). Similar to our UV-vis experiments, complex (**4**) was prepared by removing excess of dioxygen by vacuum/Ar cycles from (**2**) and careful addition of 2 mL $\bullet NO_{(g)}$ *via* 3-way gas tight syringe. Excess gas was removed by vacuum/ Ar cyles. After generation of all complexes, the tubes were frozen in $N_{2(liq)}$ and brought to the spectrometer for measurement.

Synthesis of (P^{Py})Fe^{III}-OH (5)—(P^{Py})Fe^{III}-(OH) (**5**) was prepared using a modified procedure for the synthesis of its previously published [31] chloride analog, (P^{Py})Fe^{III}-(Cl). In this case (P^{Py})Fe^{III}-(Cl) was dissolved in ~250 mL DCM, and this DCM layer was then stirred vigorously with ~250 mL of 3.0 M NaOH in a 1000 mL round-bottom flask for 3 h. Separation of the organic layer, followed by drying with magnesium sulfate, and solvent removal yielded the (P^{Py})Fe^{III}-(OH) (5) Yield 600 mg (57.8%). This compound was then characterized by UV-vis, and ^{1}H NMR spectroscopies as well as ESI-MS. UV-vis (THF): λ_{max}, nm 412, 563, room temperature. ^{1}H NMR (300 MHz; CD_2Cl_2): dpyrrole 80.63 ppm. MS (ESI): *m/z* 924. EPR g = 6.

Procedure for nitrate/nitrite test

In a 25 mL-Schlenk flask compound (**1**) was prepared in 10 mL THF (0.1 mM solution, inside dry box). In a typical bench top reaction, the flask was cooled to −80 °C (Acetone/dry ice bath) and dioxygen was bubbled through complex 1, resulting in the formation of the superoxo species, (**2**). Excess $O_{2(g)}$ was removed by several cycles of Ar bubble followed by vacuum. Addition of $\bullet NO_{(g)}$ to (2) resulted in formation of (**4**), immediately. The reaction mixture was for 10 min at −80 °C. After 10 mins, solvent was removed and solid product was isolated in 5 mL of DCM and extracted with 10 mL of aqueous NaCl solution (6 mM). The presence of a significant amount of nitrate ion in the aquous layer was confirmed by semiquantitative QUANTOFIX nitrate/nitrite test strips.

Nitration of the 2,4-di-*tert*-butylphenol (DTBP)

The formation of the superoxo complex (2) in THF at −80 °C was carried out as described above for (1) (0.1 mM) in a schlenk cuvette, and the reaction was monitored by UV-vis. Excess $O_{2(g)}$ was removed by bubbling the solution with Ar and vacuum purge cycles as before. Two equivalents of 2,4-di-tert butylphenol (DTBP) (0.1 mmol) were added. Upon addition of the DTBP no change in the UV-vis spectrum was observed. $\bullet NO_{(g)}$ was added by using a three-way gas tight syringe, leading to the formation of (5). The resulting solution

was concentrated *in vacuo* and pentane was added to precipitate the Fe product. The pentane solution was collected by decanting. The Fe product was washed several times with pentane, and the pentane solution was removed and collected by decanting after each wash. The solid Fe product (P^{Py})Fe^{III}-(S) (S = solvent, H_2O, ^-OH) was dried *in vacuo*, redissolved in THF and its UV-vis spectrum was recorded [λ_{max}= 410, 563 nm; a small change in the Soret position compared to the reaction mixture is observed, possibly due to the different solution conditions and different temperature for the spectra recorded]; these spectral parameters matched those of authentically synthesized (P^{Py})Fe^{III}(OH) (see above). The pentane solution containing the phenolic products was filtered to remove any trace of Fe product and the solvent was removed *in vacuo*. The resulting solid was re-dissolved in MeOH and dodecane used as internal standard and injected into a GC. This showed 2,4-di-*t*butyl-6-nitrophenol (NO_2-DTBP) (82% yield) and unreacted DTBP as the only products of the reaction. These were identified by comparison to the spectra obtained from commercial 2,4-di-*t*-butyl-6-nitrophenol, and 2,4-di-*t*-butylphenol respectively.

CONCLUSION

From this investigation we can conclude that our present ferric superoxo complex (2) can show cytochrome c oxidase reactivity (C*c*O) in the presence of a cuprous complex, generating a peroxo-bridged heme-Cu intermediate which can thermally transform to a heme-(O_2^-)-Cu(L) μ-oxo product, which is derived from dioxygen reactivity. Alternatively, (**2**) can also function as a •NO scavenger by oxidizing it to the biologically benign nitrate ion, complex (4). Further work is going on in our laboratory using this system.

Acknowledgements

We are grateful to the US National Institutes of Health for support of this research (GM60353).

REFERENCES

1. Holm RH, Kennepohl P, Solomon EI. Chem. Rev. 1996; 96:2239–2314. [PubMed: 11848828]
2. Perutz MF. Annu. Rev. Physiol. 1990; 52:1–25. [PubMed: 2184753]
3. Sono M, Roach MP, Coulter ED, Dawson JH. Chem. Rev. 1996; 96:2841–2888. [PubMed: 11848843]
4. English, AM.; Tsaprailis, G. Advances in Inorganic Chemistry. Sykes, AG., editor. Academic Press; 1995. p. 79-125.
5. Gardner PR, Gardner AM, Martin LA, Salzman AL. Proc. Natl. Acad. Sci. USA. 1998; 95:10378–10383. [PubMed: 9724711]
6. Wasser IM, De Vries S, Moenne–Loccoz P, Schroder I, Karlin KD. Chem. Rev. 2002; 102:1201–1234. [PubMed: 11942794]
7. Cleeter MWJ, Cooper JM, Darley-Usmar VM, Moncada S, Schapira AHV. FEBS Letters. 345:50–54. [PubMed: 8194600]
8. Brown GC, Cooper CE. FEBS Letters. 356:295–298. [PubMed: 7805858]
9. Brown GC. FEBS Letters. 369:136–139. [PubMed: 7649245]
10. Radi R. Proc. Natl. Acad. Sci. USA. 2004; 101:4003–4008. [PubMed: 15020765]
11. Szabo C, Ischiropoulos H, Radi R. Nat Rev Drug Discov. 2007; 6:662–680. [PubMed: 17667957]
12. Radi R, Beckman JS, Bush KM, Freeman BA. J. Biol. Chem. 1991; 266:4244–4250. [PubMed: 1847917]
13. Ischiropoulos H. Arch. Biochem. Biophys. 1998; 356:1–11. [PubMed: 9681984]

14. Radi R, Beckman JS, Bush KM, Freeman BA. Arch. Biochem. Biophys. 1991; 288:481–487. [PubMed: 1654835]
15. Denicola A, Freeman BA, Trujillo M, Radi R. Arch. Biochem. Biophys. 1996; 333:49–58. [PubMed: 8806753]
16. King PA, Anderson VE, Edwards JO, Gustafson G, Plumb RC, Suggs JW. J. Am. Chem. Soc. 1992; 114:5430–5432.
17. Radi R. Chem. Res. Toxicol. 1996; 9:828–835. [PubMed: 8828917]
18. Herold S, Exner M, Nauser T. Biochemistry. 2001; 40:3385–3395. [PubMed: 11258960]
19. Herold S, Shivashankar K, Mehl M. Biochemistry. 2002; 41:13460–13472. [PubMed: 12416992]
20. Kim E, Helton ME, Wasser IM, Karlin KD, Lu S, Huang HW, Moenne-Loccoz P, Incarvito CD, Rheingold AL, Honecker M, Kaderli S, Zuberbuhler AD. Proc. Natl. Acad. Sci. USA. 2003; 100:3623–3628. [PubMed: 12655050]
21. Kim E, Chufan EE, Kamaraj K, Karlin KD. Chem. Rev. 2004; 104:1077–1133. [PubMed: 14871150]
22. Chufan EE, Puiu SC, Karlin KD. Acc. Chem. Res. 2007; 40:563–572. [PubMed: 17550225]
23. Halime Z, Kieber-Emmons MT, Qayyum MF, Mondal B, Gandhi T, Puiu SC, Chufan EE, Sarjeant AA, Hodgson KO, Hedman B, Solomon EI, Karlin KD. Inorg. Chem. 2010; 49:3629–3645. [PubMed: 20380465]
24. Halime Z, Kotani H, Li Y, Fukuzumi S, Karlin KD. Proc. Natl. Acad. Sci. USA. 2011; 108:3990–3994.
25. Ferguson-Miller S, Babcock GT. Chem. Rev. 1996; 96:2889–2908. [PubMed: 11848844]
26. Tsukihara T, Aoyama H, Yamashita E, Tomizaki T, Yamaguchi H, Shinzawa-Itoh K, Nakashima R, Yaono R, Yoshikawa S. Science. 1995; 269:1069–1074. [PubMed: 7652554]
27. Iwata S, Ostermeier C, Ludwig B, Michel H. Nature. 1995; 376:660–669. [PubMed: 7651515]
28. Varotsis C, Zhang Y, Appelman EH, Babcock GT. Proc. Natl. Acad. Sci. USA. 1993; 90:237–241. [PubMed: 8380495]
29. Collman JP, Sunderland CJ, Berg KE, Vance MA, Solomon EI. J. Am. Chem. Soc. 2003; 125:6648–6649. [PubMed: 12769571]
30. Momenteau M, Reed CA. Chem. Rev. 1994; 94:659–698.
31. Li Y, Sharma SK, Karlin KD. Polyhedron. 2013; 58:190–196.
32. Liang HC, Zhang CX, Henson MJ, Sommer RD, Hatwell KR, Kaderli S, Zuberbuhler AD, Rheingold AL, Solomon EI, Karlin KD. J. Am. Chem. Soc. 2002; 124:4170–4171. [PubMed: 11960420]
33. Kieber-Emmons MT, Qayyum MF, Li Y, Halime Z, Hodgson KO, Hedman B, Karlin KD, Solomon EI. Angew. Chem. Int. Ed. Engl. 2012; 51:168–172. [PubMed: 22095556]
34. Kieber-Emmons MT, Li Y, Halime Z, Karlin KD, Solomon EI. Inorg. Chem. 2011; 50:11777–11786. [PubMed: 22007669]
35. Chufan EE, Mondal B, Gandhi T, Kim E, Rubie ND, Moenne-Loccoz P, Karlin KD. Inorg. Chem. 2007; 46:6382–6394. [PubMed: 17616124]
36. Del Rio D, Sarangi R, Chufan EE, Karlin KD, Hedman B, Hodgson KO, Solomon EI. J. Am. Chem. Soc. 2005; 127:11969–11978. [PubMed: 16117536]
37. Kim E, Helton ME, Lu S, Moenne-Loccoz P, Incarvito CD, Rheingold AL, Kaderli S, Zuberbuhler AD, Karlin KD. Inorg. Chem. 2005; 44:7014–7029. [PubMed: 16180864]
38. Karlin KD, Nanthakumar A, Fox S, Murthy NN, Ravi N, Huynh BH, Orosz RD, Day EP. J. Am. Chem. Soc. 1994; 116:4753–4763.
39. Sharma V, Karlin KD, Wikström M. Proc. Natl. Acad. Sci. USA. 2013; 110:16844–16849. [PubMed: 24082138]
40. Fox S, Nanthankumar A, Wikstrom M, Karlin KD, Blackburn NJ, et al. J. Am. Chem. Soc. 1996; 118:24–34.
41. Ghiladi RA, Karlin KD. Inorg. Chem. 2002; 41:2400–2407. [PubMed: 11978105]

42. Ghiladi RA, Huang H-W, Moenne-Loccoz P, Stasser J, Blackburn NJ, Woods AS, Cotter RJ, Incarvito CD, Rheingold AL, Karlin KD. J. Biol. Inorg. Chem. 2005; 10:63–77. [PubMed: 15583964]
43. Ghiladi RA, Chufan EE, Rio DD, Solomon EI, Kerbs C, Huynh BH, Huang H-W, Moenne-Loccoz P, Kaderli S, Honecker M, Zuberbuhler AD, Marzilli L, Cotter RJ, Karlin KD. Inorg. Chem. 2007; 46:3889–3902. [PubMed: 17444630]
44. Schopfer MP, Mondal B, Lee DH, Sarjeant AA, Karlin KD. J. Am. Chem. Soc. 2009; 131:11304–11305. [PubMed: 19627146]
45. Olson JS, Foley EW, Rogge C, Tsai AL, Doyle MP, Lemon DD. Free Radic. Biol. Med. 2004; 36:685–697. [PubMed: 14990349]
46. Yukl ET, De Vries S, Moenne-Loccoz P. J. Am. Chem. Soc. 2009; 131:7234–7235. [PubMed: 19469573]
47. Herold S, Koppenol WH. Coord. Chem. Rev. 2005; 249:499–506.
48. Gunaydin H, Houk KN. J. Am. Chem. Soc. 2008; 130:10036–10037. [PubMed: 18613683]
49. Pacher P, Beckman JS, Liaudet L. Physiol. Rev. 2007; 87:315–424. [PubMed: 17237348]
50. Boccini F, Herold S. Biochemistry. 2004; 43:16393–16404. [PubMed: 15610034]
51. Kurtikyan TS, Eksuzyan SR, Goodwin JA, Hovhannisyan GS. Inorg. Chem. 2013; 52:12046–12056. [PubMed: 24090349]

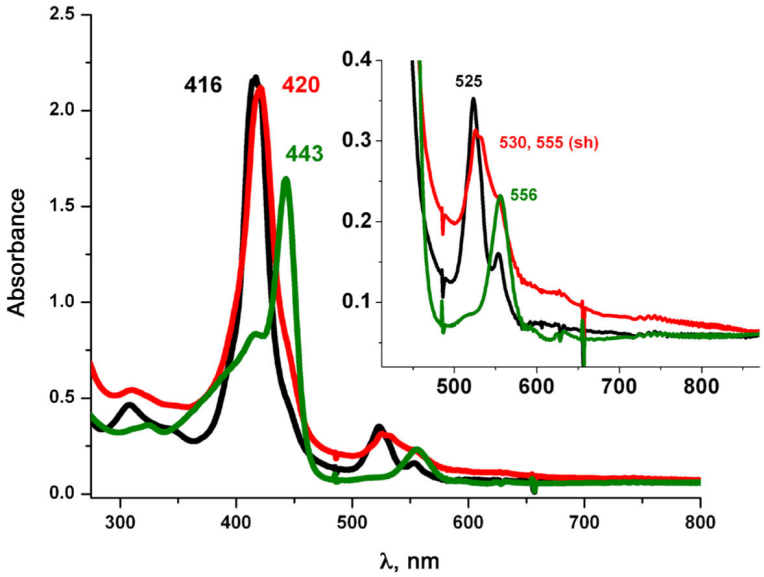

Fig. 1.

UV-vis spectra of (1, black) a reduced $(P^{Py})Fe^{II}$ + $[Cu^{I}(AN)]^{+}$ 1:1 mixture; (**3a**, red) high spin peroxo complex $[(P^{Py})Fe^{III}\text{-}(O_2^{2-})\ Cu^{II}(AN)]^{+}$; (**3**, green) μ-oxo complex $[(P^{Py})Fe^{III}\text{-}(O^{2}\text{-})\text{-}Cu^{II}(AN)]^{+}$

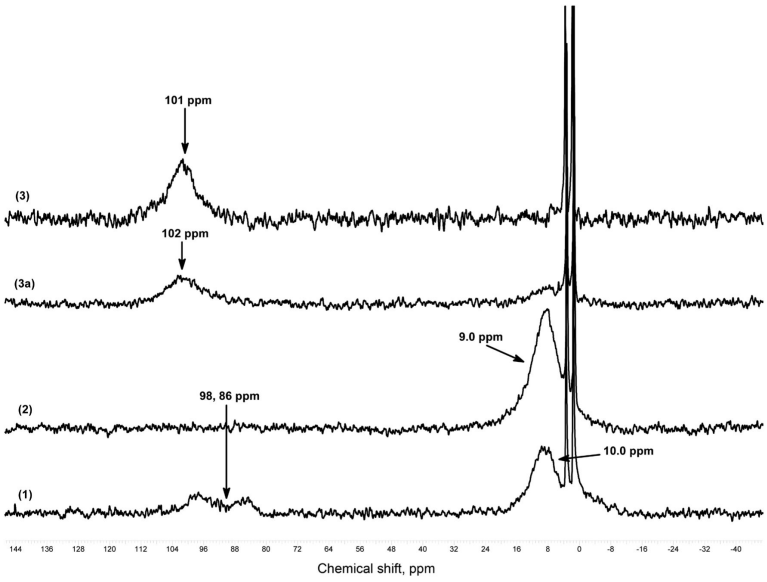

Fig. 2.

^{2}H NMR spectra at −80 °C in THF (1) (d_8-P^{Py})Fe^{II}-THF, (2) (d_8-P^{Py})Fe^{III}-(O_2^{2-}) (**3a**) [(d_8-P^{Py})Fe^{III}-(O^2)-Cu^{II}(AN)]$^+$ and (**3**) [(d_8-P^{Py})Fe^{III}-(O_2-)-Cu^{II}(AN)]$^+$

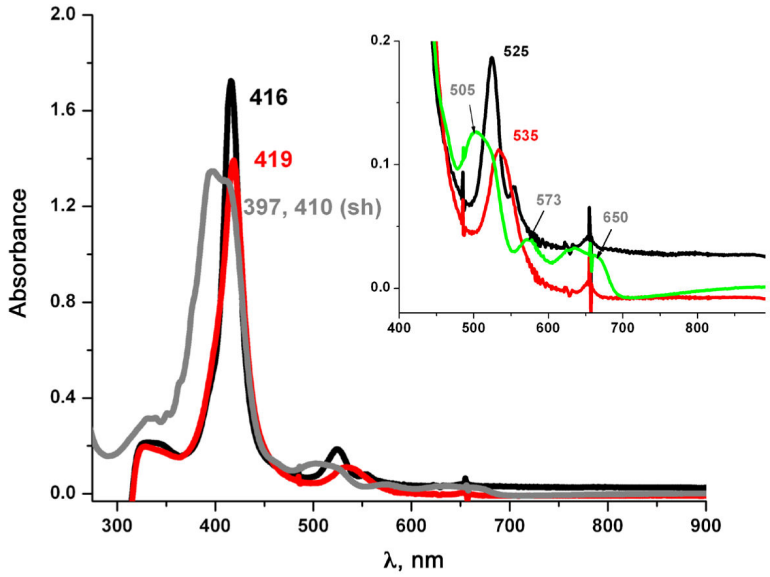

Fig. 3.

UV-vis spectra showing superoxo (**2**, red) formed from reduced (P^{Py})FeII (1, black) by bubbling $O_{2(g)}$ at −80 °C; nitrato complex (P^{Py})Fe^{III}-ONO_2 (**4**, grey) generated immediately after addition of •$NO_{(g)}$

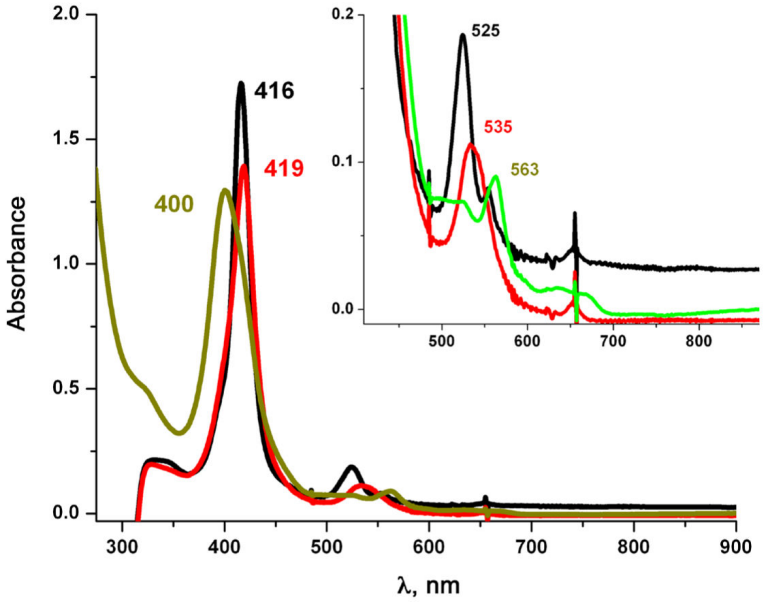

Fig. 4.

UV-vis spectroscopy in THF at −80 °C. The black spectrum is reduced (P^{Py})Fe^{II} (1); red is (2 + DTBP), and green is (5)

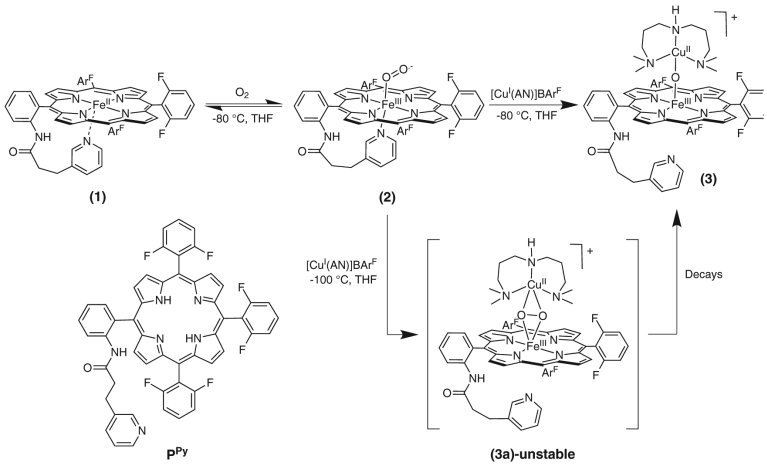

Scheme 1.

Formation of $(P^{Py})Fe^{III}$-$(O_2^{\bullet-})$ (2) *via* oxygenation of $(P^{Py})Fe^{II}$ (**1**) and subsequent reaction with $[Cu^{I}(AN)]^{+}$ to give the meta-stable intermediate, the high-spin heme-peroxo-copper complex (**3a**), which decays to give the m-oxo complex $[(P^{Py})Fe^{III}$-(O_2^{-})- $Cu^{II}(AN)]^{+}$ (**3**)

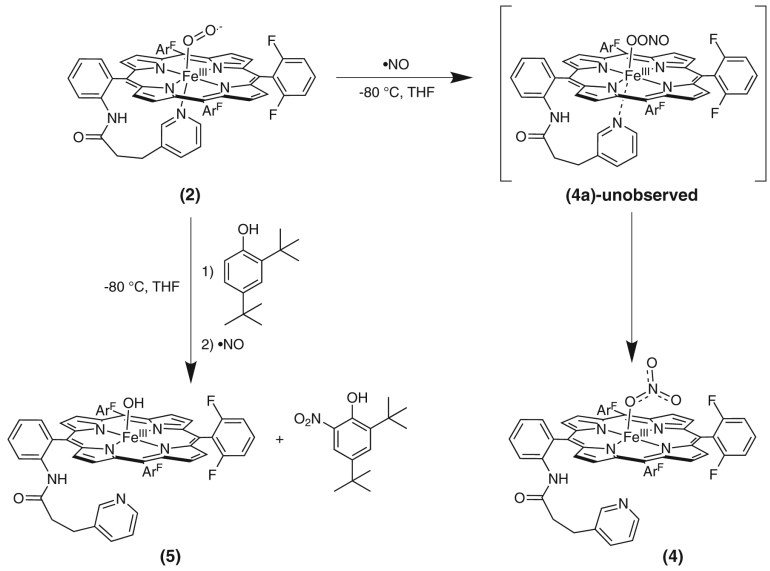

Scheme 2.

Reaction sequence where $\bullet NO_{(g)}$ is added to superoxo complex (**2**) to give nitrato complex (**4**). In the presence of a phenolic substrate, the same reaction gives (**5**) as a final product along with the *ortho*-nitrated phenol